Cerebrospinal Fluid Velocity Amplitudes within the Cerebral Aqueduct in Healthy Children and Patients with Chiari I Malformation

This is the author manuscript accepted for publication and has undergone full peer review but has not been through the copyediting, typesetting, pagination and proofreading process, which may lead to differences between this version and the Version record. Please cite this article as doi:10.1002/jmri.25160.

ABSTRACT

***PURPOSE*:** To assess the effects of cerebrospinal fluid (CSF) bidirectional motion in Chiari malformation type I (CMI), we monitored CSF velocity amplitudes on phase contrast MRI (PC-MRI) in patients before and after surgery; and in healthy volunteers.

***METHODS*:** 10 pediatric volunteers and 10 CMI patients participated in this study. CMI patients underwent PC-MRI scans before and approximately 14 months following surgery. Two parameters—amplitude of mean velocity (AMV) and amplitude of peak velocity (APV) of CSF—were derived from the data. Measurements were made at the mid-portion of the cerebral aqueduct; and anterior and posterior compartments of the spinal canal at the craniovertebral junction (CVJ).

***RESULTS*:** AMV and APV within the cerebral aqueduct were greater in preoperative assessments of the CMI patients compared to normal volunteers. Statistical significance was noted when comparing aqueductal AMV between the preoperative values and normal controls ($p=0.03$); and before and after surgery in the CMI patients ($p=0.02$). Lower values of AMV ($p= 0.02$) were noted in the anterior CVJ compartment in the patients before and after surgery when compared to the normal volunteers. There were no significant correlations ($p= 0.06$) noted for the APV at the CVJ between the normal control and patients, before or after surgery.

***CONCLUSIONS*:** In pediatric CMI patients, AMV for CSF within the cerebral aqueduct and anterior CVJ subarachnoid space are significantly elevated preoperatively and normalize following surgery. Given the biphasic CSF motion, measuring amplitude accounts for cranial and caudal flow .It may offer an alternative parameter to assess postsurgical outcome.

***Key words*:** Cerebrospinal fluid; Chiari malformation; cerebral aqueduct; MRI phase contrast imaging.

INTRODUCTION

Chiari malformation type I (CMI*)* is associated with abnormal cerebrospinal fluid (CSF) motion within the craniovertebral junction (CVJ) subarachnoid space (1,2). Cerebellar tonsillar position 5 mm or more below the foramen magnum is the most widely accepted imaging criterion for the diagnosis of CMI (3-5). For patients with symptomatic CMI, surgical decompression is the treatment of choice (6,7). However, in many cases the decision to recommend surgical treatment is not clear and a subset of patients who undergo surgical decompression surgery do not achieve symptomatic relief (8). We focused our studies to a cohort of pediatric patients, who form the single largest group of patients who undergo definitive decompression surgery for CMI.

Given that an improved understanding of the CMI pathophysiology may lead to the identification of diagnostic tools that can more specifically predict the surgical outcome, the purpose of this study was to develop a parameter to better characterize the CSF flow alterations in pediatric patients presenting with CMI. Previous studies have focused on measurements at the foramen magnum, a location that is ill-defined after suboccipital craniectomy. Further, PC-MRI flow measurements at the CVJ can be complicated by velocity aliasing artifacts from the vertebral arteries. Studies have in the past focused on evaluation of mean or peak velocities and have not taken into consideration the bi-directional flow of CSF. In this study, we evaluated using the parameter of amplitude of the peak and mean flow, which appears to be more robust in assessing CSF flow. We focused our attention on flow measurements at the cerebral aqueduct (AS), which is untouched and pristine following decompression surgery at the CVJ. Peak velocity measurement at the AS is free of aliasing artifacts from vascular structures and surgical alterations, and therefore has attracted the attention of investigators such as Liu et al (9) and Wang et al (10), though with conflicting results. The former study showed increased cranial and caudal peak

velocities at the aqueduct in pre-surgical evaluations of adult CMI patients, and the latter study showed decreased cranial peak velocities and increased caudal peak velocities in a similar cohort. In this study, we hypothesized that the cranio-caudal amplitude of CSF flow can better characterize the CSF flow alterations in pediatric CMI patients than peak CSF velocities.

METHODS

Approval of this study was granted by the Institutional Review Board. Written informed consent and parental assent, when required, were obtained from all subjects.

Study Population

Ten normal healthy pediatric volunteers were recruited via the University of Michigan's ENGAGE website. Ten CMI patients were referred from the Department of Neurosurgery. The inclusion criteria for the patients were: worsening headache, symptoms altering daily life activities, and/or presence of spinal syrinxes, which were also the indications of Chiari decompression at our institution. The exclusion criteria were: CMI patients with hydrocephalus, adult CMI patients above the age of 21 years, and patients with previous history of surgical decompression for CMI. PC-MRI CSF velocity measurements were not used by the surgeon to determine candidacy for surgical treatment. All CMI patients underwent suboccipital craniotomy with removal of the posterior arch of the C1 vertebra. Six patients had duraplasty with a patch graft. The tonsils were coagulated in five patients. All patients were prospectively followed with clinical and imaging assessments, and the outcome of the surgery was evaluated using the 16-point Chicago Chiari Outcome Scale (11). The CSF flow studies were repeated approximately 14 months after surgery in the CMI patients.

Imaging Parameters

Ten healthy volunteers were prospectively evaluated on a 3 Tesla MRI scanner (Philips Medical Systems, Eindhoven, Netherlands). The volunteers were not sedated. PC-MRI (CSF flow) scans were obtained using the following parameters: repetition time (TR) / echo time (TE) = 21/10.6 ms, # averages = 1, flip angle =10° , field of view = 250×180 mm^2, matrix = 512×512, slice thickness = 5 mm, resolution= 0.49 mm, scan time = 2:00 minutes, readout bandwidth

=225 Hz/pixel, and parallel acceleration factor = 2. Fifteen timeframes were collected during each cardiac cycle (using a peripheral-pulse unit (PPU) signal with retrospective triggering), providing a temporal resolution of about 52.6 ms (for an average heart rate of 75 beats per minute (bpm)). The scans were obtained in the sagittal position (localization scans) and perpendicular to CSF flow direction (through-plane velocity-encoding PC-MRI scans) at the CVJ and also through the cerebral aqueduct. The scans were performed with the neck in neutral position. The chin was taped down and secured for imaging.

Ten symptomatic CMI patients were scanned both pre- and post-operatively utilizing either 1.5 or 3 Tesla MRI scanner. The same field strength scanner was used for all scans obtained on any given patient. The imaging parameters for the sequences on the 3T scanner were the same as previously described. The imaging parameters on the 1.5T scanner were: TR/TE = 19.2/ 7.7 ms, #averages = 1, flip angle = 15º, field of view = 208×145 mm^2, matrix = 256×256, slice thickness = 4 mm , scan time = 3.20 minutes and readout bandwidth = 184 Hz/pixel. Sixteen timeframes were collected during each cardiac cycle, providing a temporal resolution of about 50 ms (for an average heart rate of 75 bpm). The chin was taped down and secured for imaging. The patients were not sedated.

The location, orientation, and region-of-interest (ROI) of the conducted scans are illustrated in Figures 1 and 2. CSF flow measurements at the aqueduct were carried in a similar manner in the patients and normal controls. Flow measurements within the AS were measured in a plane perpendicular to the midpoint of a line joining cranial and caudal ends of the aqueduct on sagittal images

CSF flow at the CVJ in normal volunteers was measured in the axial plane corresponding to the McRae line. In order to have corresponding flow measurements in patients and normal volunteers, flow was measured at the CVJ in the patients by setting the imaging plane just below

the tip of the cerebellar tonsil. This also ensured that the flow measurements could be obtained posterior to the spinal cord and free from any confounding signals from the vertebral arteries or the descended tonsils. The selected axial plane was oriented such that the central cursor was parallel to the CSF space anterior to the spinal cord on a sagittal T1-weighted image. The scans were carefully monitored by two investigators (FL and JRB) for all studies and each time, to minimize variations in the scan plane selection. The two investigators worked together and corroborated the results. In the patients, the location of the scan plane was replicated using the reference plane of the C2-C3 disc space and the length of the odontoid, given that the posterior arch of the C1 vertebra was not available in the post-operative evaluations.

VENC Selection

PC-MRI is based on manipulating the imaging pulse sequence with a bipolar gradient. Stationary tissues are not affected by the bipolar gradient as the phase gained by the spins during the positive lobe of the gradient is lost during the negative lobe. However, for moving spine, there will be a phase difference between the phase gained during the positive gradient lobe and that lost during the negative gradient lobe, such that the phase difference depends on the tissue velocity. The velocity-encoding (VENC) parameter is adjusted in the imaging protocol to be slightly higher than the maximum expected velocity, which ensures that the maximum accumulated phase does not exceed 2π, thus avoiding velocity aliasing artifacts. In this study, VENC was optimized for each subject and ranged from 5 to 12 cm/s in the through-plane R1-direction perpendicular to the CSF flow direction. The smallest VENC value that does not cause aliasing was chosen for final analysis. The aliasing artifacts were avoided by reviewing each scan immediately after acquisition and repeating the scan as necessary (e.g., at a higher VENC value with VENC changes increased in increments of 2 cm/s). Two authors (FJL and JRB) performed all measurements and image analysis, including ROI placement and closely

monitoring the studies.

Flow Measurements and Analysis

All CSF flow sequences were analyzed using the Medis Q-Flow software (Medis, Leiden, The Netherlands). This software prompts the user to define a ROI in the subarachnoid space in the phase images (Figure 2 b and c). For CVJ CSF velocity measurement, elliptical ROIs were drawn in the axial imaging plane. Two ovoid compartments were identified, one anterior and one posterior to the visualized denticulate ligament. Particular care was taken to exclude pixels that included vessels (e.g., vertebral arteries). For the cerebral aqueduct CSF measurements, one circular-shaped ROI was drawn over the cross-section of the aqueduct. All ROI's were edited to include only CSF containing pixels.

The Q-Flow software exported the results to an Excel spreadsheet (Microsoft Corp., Redmond, WA) with the following data for each phase of the cardiac cycle: 1) trigger delay; 2) flux (ml/s); 3) area; 4) pixel count; 5) mean velocity; 6) maximum velocity in the cephalic direction; 7) minimum velocity in the cephalic direction (i.e., maximum caudal velocity); 8) peak velocity; and 9) velocity standard deviation. Each PC-MRI scan produced 15 time points (measurements) for normal volunteers and 16 time points for patients. These time points were of two types, average or peak, where "average" refers to the average signal intensity of each pixel that comprises the ROI, and "peak" is the maximum signal intensity pixel within that ROI. The peak measurements define "jets" of the CSF motion, while the average measurements reduce them. Amplitude of mean velocity (AMV) was defined as the difference between cranial and caudal mean velocities within the entire ROI. Amplitude of peak velocity (APV) was defined as the difference between maximum numerical value of cranial versus caudal CSF velocity for any pixel within the ROI over the cardiac cycle (Figure 2 a). For each scan, CSF, APV, and AMV within a ROI were calculated. The results were compared in terms of the mean

and standard deviation for each group.

Demographics

Of the normal volunteers, 4 were males and 6 were females with a mean age of 11±2.4 years. Of the 10 CMI patients, 6 were males and 4 were females. The CMI patients had preoperative MRI scans at a mean age of 13.5±4.5 years. The demographics by age of normal volunteers and patients at the time of their pre-operative and post-operative scans are shown in Table 3. The mean time interval between pre- and post-operative MRI scans was 19.5 months. The post-operative studies were carried out approximately 14 months after surgery.

Statistical Analysis

Normalized cerebrospinal fluid flow in the post-surgical flow studies inpatients was analyzed as an outcome measure for evaluating improvement in patients' symptoms following decompression surgery. Continuous variables were summarized as means and standard deviations. Baseline normalized CSF was compared between normal volunteers and CMI patients by using student's t-test. A paired t-test was used to compare the pre- and post-surgery normalized flow for CMI patients. A p value of 0.05 or smaller was considered significant for all hypothesis tests. The above procedures were done in Excel (Microsoft Corp., Redmond WA 2010).

RESULTS

Table 1 summarizes the CSF velocity measurements for the volunteers and CMI patients, including APV and AMV within the cerebral aqueduct and within CVJ subarachnoid space.

The amplitudes of CSF velocities at the AS range from 8.8±3.4 cm/s (the highest preoperative APV) to 1.7 ± 2.4 cm/s (the lowest postoperative AMV). Within the cerebral aqueduct, APV trended higher, but not significant, in the CMI patients compared to the normal volunteers (8.8±3.4cm/s vs. 6.6±2.3 cm/s; p=0.11). The APV returned to 6.4±2.5 cm/s post-operatively. Within the cerebral aqueduct, the AMV was significantly higher in preoperative CMI patients compared to the normal volunteers (3.8±1.4 cm/s vs. 2.6±0.9 cm/s; p=0.03). Post-operatively, there was no statistical difference from the normal volunteers (p = 0.63) (Table 2; Figure 3).

Within the anterior CVJ subarachnoid space, preoperative CMI patients had a higher APV than volunteers (11.1±8.0 cm/s vs. 10.7±2.0 cm/s) that decreased to 8.5±4.2 cm/s after surgery, with neither differences being statistically significant.

At the anterior CVJ subarachnoid space, the AMV was lower in the pre-operative CMI patients compared to normal volunteers (4.3±1.6 cm/s vs. 6.1±1.2 cm/s; p=0.01). Post-operatively, AMV remained lower (1.2±5.7 cm/s). Within the posterior CVJ subarachnoid space, there was no statistically significant difference between the three groups for APV or AMV (Table 3).

Nine patients presented with headache. One patient presented with right-arm weakness and pain. Four patients presented with complaints including snoring, right extremity weakness, facial weakness, and neck pain. Four patients had a syrinx. Headache completely resolved in 7 of 9 patients post-operatively; 2 patients complained of occasional, but substantially improved, headaches postoperatively. Of the 4 patients with syrinxes diagnosed

pre-operatively, one syrinx completely resolved post-operatively and 3 showed significant decrease in size. Post-operatively, all other neurological symptoms either resolved or were significantly improved. There were no post-operative complications. Using the Chicago Chiari Outcome Scale (11), 7 patients scored 16 and 3 patients scored 15. Table 4 summarizes the clinical presentations, operations and surgical outcomes.

DISCUSSION

MRI is the only technique available for non-invasive analysis of CSF movement (12). Net movement of CSF in the cerebral aqueduct over time is caudal due to CSF production in the brain ventricles and absorption in the subarachnoid space. Despite this net caudal movement, each pulse cycle generally has a period of cranial as well as caudal CSF movement within the cerebral aqueduct. Both phases may be combined as a single flow value for each cardiac cycle. In the reported measurements by the Q-flow software in this study, the net flow at the AS of every scan was 0 ml/s. In comparison, the range of values for the measurement of amplitudes offers a more illustrative and objective assessment of CSF motion. It is not difficult to imagine a scenario where large changes in amplitude were coupled with no or only a minor change in net flow. In our study, statically significant changes in amplitude were seen without any change in net flow. Therefore, in this study, we chose to use amplitudes of flow (AMV and APV) to assess CSF hydrodynamics, which we believe represents a more robust measurement of bidirectional CSF motion (APV illustrates flow "jets" and AMV relates to mean velocity of the bidirectional motion of CSF fluid during a cardiac cycle (13)).

The importance of aqueductal CSF velocities has been previously highlighted in the literature (14). We chose cerebral aqueduct CSF measurements as an independent prognostic marker to assess the CSF motion alterations before and after the CMI decompression surgery, because the aqueduct is not affected by surgical decompression which does change the morphology and geometry of the CVJ.

From the data reported by Wang et al, we extrapolated and calculated the APV at the aqueduct in preoperative CMI patients to be 5.71 cm/s compared to 5.59 cm/s in volunteers, and 5.68 cm/s after posterior fossa decompression. A similar decrease in amplitude is observed when the APVs are calculated from the data published by Liu et al (preoperative patients: 7.73

cm/s, volunteers: 4.24 cm/s). The apparent discordance between the findings by Wang et al. and by Liu et al. is reconciled when their APV values are compared. Similarly, our own data suggest a decreasing trend for APV at the AS after decompression (p=0.09). These observations strengthen our view that the amplitude of velocity is useful to help assess measurement of the CSF flow dynamics. In another review of CSF flow dynamics in CMI, (15) were no changes in APV at the AS after decompression. The highly variable APV observed by this group may be explained by their highly heterogeneous study population, with patients ranging from 3 to 80 years of age.

Critical evaluations of CSF flow in the cerebral aqueduct by previous investigators have demonstrated that the CSF velocity at the cerebral aqueduct varies with age (16-19). We have any bias that may be introduced in our study by limiting our study to an adolescent pediatric population, with as little variation in age as possible, to minimize age as a confounding factor. A larger cohort study is planned to assess aqueduct flow amplitudes over a wider age range in a pediatric cohort.

The previously described observations for the tendency for peak velocities to increase from the rostral aspect to the caudal aspect of the cerebral aqueduct (18) was mitigated by standardizing our technique to measure the flow at the mid-point of the cerebral aqueduct.

Analyses of the CSF amplitude parameters in the anterior CVJ subarachnoid space revealed statistically significant differences in the AMV measurements between normal volunteers and post-operative patients. It is important to note that the degree of reduction of the flow amplitude in this space closely resembles that of the cerebral aqueduct. Given the significant morphological alterations in the posterior subarachnoid space following decompression surgery, it is this anterior portion of the spinal subarachnoid space that is less likely to be affected by the surgical procedure, similar to the aqueduct.

Assessment of the posterior subarachnoid space at the CVJ revealed no significant differences in CSF flow amplitudes in this study. Complexity of the CSF flow in this space is governed by change in the geometry of the space and is less homogeneous compared to the cerebral aqueduct. Therefore, we believe that the CSF measurements in this space will yield ambiguous results. Additionally, the inherent pulsations of the spinal cord and cerebellar tonsils or their remnants during the cardiac cycle may obscure and possibly even negate any possible significant changes that might be attributed to velocity assessments of the subarachnoid space at the CVJ.

Comparing pre-operative and post-operative hydrodynamics of a subarachnoid space that has been altered in morphology by interval surgery can be confounding. This is particularly true if one is only measuring net flow, which is usually close to zero. By assuming the apparent, generalized intracranial relationship of CSF motion, we were able to compare the dynamic amplitude of CSF motion of the unaltered (by the interval CVJ surgery) cerebral aqueduct to its pre-operative CSF motion with the assurance that whatever differences we observed were not due to local anatomic post-operative changes. Since all CMI patients in this study were symptomatic, we do not know if this observed increase in amplitude of CSF motion occurs in asymptomatic CMI patients, or is only present in symptomatic CMI patients. However, we can state that in our study, the post-surgical group had both normal motion amplitudes and symptomatic improvement.

At the CVJ, there was no significant change of either amplitude parameter comparing controls to pre- and post-operative groups in either the anterior or posterior subarachnoid spaces. Post-surgical APV non-significantly increased in the posterior space. This suggests that surgical intervention had no impact on CSF motion in these regions. We surmise that alterations of CSF flow in these subarachnoid spaces were obscured by changes related to the

interval decompression surgery and that measurements obtained from the aqueduct better reflect the true impact of surgery on CSF motion.

Following surgery, there was no statistical differences between post-surgery and volunteer groups, thereby indicating "normalization" of flow amplitude postoperatively. While the decrease in CSF flow might be explained by an interval increase in the aqueduct diameter, this is unlikely, as the decompression surgery was performed at the CVJ. Alternatively, and more plausibly, we believe that surgery at the CVJ changes CSF dynamics, which alters intracranial compliance in a way that results in diminished aqueductal CSF flow. This is supported by the theory that the pulse-absorber characteristics of the cranio-spinal system (20-22) may play an important role in CSF hydrodynamics in CMI patients.

The major limitation of our study is the small numbers of both volunteers and symptomatic patients. In the future, larger patient and control cohorts will be necessary to emphatically validate our conclusions.

Another limitation of our study is that all CMI patients included in this analysis were symptomatic. All patients were considered to be surgical candidates pre-operatively and had good surgical outcomes. The results of this study might not apply to asymptomatic patients with low cerebellar tonsil position (23). We did not take into account any alterations in the cross-sectional area in the posterior CVJ due to the difficulty of accurately selecting the ROI in the geometrically complex post-surgical subarachnoid space. Selection of a ROI at the CVJ can be problematic as the location of the foramen magnum, becomes obscured after suboccipital craniectomy. For this reason, we selected our ROI in the axial plane just below the tip of the cerebellar tonsil. Because the cerebellar tonsils are lower in CMI, the ROI is selected lower than in normal patients. The length of the odontoid and the C2-C3 disc space then served as a landmark to accurately place the plane of axial imaging for the phase contrast sequence in the post-

surgical scans.

Surgical procedures were not uniform in this series; patients were treated, either with or without duraplasty which did not allow for comparison between these 2 "surgical" sub-groups.

There were necessary minor variations in the scan parameters between normal volunteers and patients that we believe did not influence the quantitative analysis. In this study, since all CMI patients had good post-operative outcomes, we are unable to definitively conclude that the high CSF flow indices observed within the aqueduct are a pre-operative indicator of surgical success. A larger diverse cohort of pediatric patients will be needed to investigate whether aqueductal CSF velocity can identify CMI patients who may develop a spinal cord syrinx, will eventually develop certain specific symptoms, and/or respond positively to surgery.

While it is known that CSF flow at the craniovertebral junction is age dependent and evolves during the first 2 decades of life (possibly related to tonsillar ascent), the small size of our patient/volunteer group precluded evaluation of pre-operative versus post-operative flow changes as a function of patient age. Similarly, while 4 of our patients had pre-operative cervical spinal cord syrinx cavities (all of which improved/resolved post-operatively), no conclusions can be reached or even suggested about the importance of these findings again due to the small size of our patient population. However, we believe that using aqueductal velocities as opposed to CSF junction velocities obviates concerns about the effect of operative tonsillar coagulation.

In conclusion, the amplitude of the mean and peak velocities (AMV and APV, respectively) within the CVJ subarachnoid space and within the cerebral aqueduct measured in a cohort of symptomatic CMI patients were generally higher in the CMI patients compared to healthy subjects. These parameters in CMI patients tended to revert to values similar to normal healthy subjects following clinically successful CVJ decompression surgery. As measurements at the

CVJ may be confounded by post-operative change, it appears that preoperative elevations of AMV CSF motion *in the cerebral aqueduct* may be the better parameter to identify abnormal CSF dynamics in symptomatic CMI patients who might ultimately benefit from decompressive surgery. Further study of larger symptomatic and asymptomatic CMI patient groups is warranted.

***Conflict of interest statement*:**

All authors (JRB, FJL, ND, COM, BAM, HJLG, KAM, EIH, DJQ) do not have any financial relationship with the organization which gave grant support to this research project. All authors (JRB, FJL, ND, COM, BAM, HJLG, KAM, EIH, DJQ) declare that they have no conflict of interest.

REFERENCES

1. Oldfield EH, Muraszko K, Shawker TH, Patronas NJ. Pathophysiology of syringomyelia associated with Chiari I malformation of the cerebellar tonsils. Implications for diagnosis and treatment. Journal of neurosurgery 1994;80(1):3-15.
2. Shaffer N, Martin B, Loth F. Cerebrospinal fluid hydrodynamics in type I Chiari malformation. Neurological research 2011;33(3):247-260.
3. Barkovich AJ, Wippold FJ, Sherman JL, Citrin CM. Significance of cerebellar tonsillar position on MR. AJNR American journal of neuroradiology 1986;7(5):795-799.
4. Mikulis DJ, Diaz O, Egglin TK, Sanchez R. Variance of the position of the cerebellar tonsils with age: preliminary report. Radiology 1992;183(3):725-728.
5. Smith BW, Strahle J, Bapuraj JR, Muraszko KM, Garton HJ, Maher CO. Distribution of cerebellar tonsil position: implications for understanding Chiari malformation. Journal of neurosurgery 2013;119(3):812-819.
6. Ellenbogen RG, Armonda RA, Shaw DW, Winn HR. Toward a rational treatment of Chiari I malformation and syringomyelia. Neurosurgical focus 2000;8(3):E6.
7. Tubbs RS, Beckman J, Naftel RP, et al. Institutional experience with 500 cases of surgically treated pediatric Chiari malformation Type I. Journal of neurosurgery Pediatrics 2011;7(3):248-256.
8. Tubbs RS, McGirt MJ, Oakes WJ. Surgical experience in 130 pediatric patients with Chiari I malformations. Journal of neurosurgery 2003;99(2):291-296.
9. Liu B, Wang ZY, Xie JC, Han HB, Pei XL. Cerebrospinal fluid dynamics in Chiari malformation associated with syringomyelia. Chinese medical journal 2007;120(3):219-223.

0. Wang CS, Wang X, Fu CH, Wei LQ, Zhou DQ, Lin JK. Analysis of cerebrospinal fluid flow dynamics and morphology in Chiari I malformation with cine phase-contrast magnetic resonance imaging. Acta neurochirurgica 2014;156(4):707-713.
1. Aliaga L, Hekman KE, Yassari R, et al. A novel scoring system for assessing Chiari malformation type I treatment outcomes. Neurosurgery 2012;70(3):656-664; discussion 664-655.
2. Menick BJ. Phase-contrast magnetic resonance imaging of cerebrospinal fluid flow in the evaluation of patients with Chiari I malformation. Neurosurgical focus 2001;11(1):E5.
3. Chen M-Y, Huang T-Y, Chen C-Y, Chung H-W. The significance of net CSF flow at the cerebral aqueduct: a cine phase-contrast study (poster #1678). International Society for Magnetic Resonance in Medicine Proceedings. Denver, CO; 2000.
4. Kolbitsch C, Schocke M, Lorenz IH, et al. Phase-contrast MRI measurement of systolic cerebrospinal fluid peak velocity (CSFV(peak)) in the aqueduct of Sylvius: a noninvasive tool for measurement of cerebral capacity. Anesthesiology 1999;90(6):1546-1550.
5. Mauer UM, Gottschalk A, Mueller C, Weselek L, Kunz U, Schulz C. Standard and cardiac-gated phase-contrast magnetic resonance imaging in the clinical course of patients with Chiari malformation Type I. Neurosurgical focus 2011;31(3):E5.
6. Stoquart-ElSankari S, Baledent O, Gondry-Jouet C, Makki M, Godefroy O, Meyer ME. Aging effects on cerebral blood and cerebrospinal fluid flows. Journal of cerebral blood flow and metabolism : official journal of the International Society of Cerebral Blood Flow and Metabolism 2007;27(9):1563-1572.
7. Unal O, Kartum A, Avcu S, Etlik O, Arslan H, Bora A. Cine phase-contrast MRI evaluation of normal aqueductal cerebrospinal fluid flow according to sex and age. Diagnostic and interventional radiology 2009;15(4):227-231.

8. Lee JH, Lee HK, Kim JK, Kim HJ, Park JK, Choi CG. CSF flow quantification of the cerebral aqueduct in normal volunteers using phase contrast cine MR imaging. Korean journal of radiology : official journal of the Korean Radiological Society 2004;5(2):81-86.

9. Luciano M, Dombrowski S. Hydrocephalus and the heart: interactions of the first and third circulations. Cleveland Clinic journal of medicine 2007;74 Suppl 1:S128-131.

0. Park EH, Dombrowski S, Luciano M, Zurakowski D, Madsen JR. Alterations of pulsation absorber characteristics in experimental hydrocephalus. Journal of neurosurgery Pediatrics 2010;6(2):159-170.

1. Wagshul ME, Eide PK, Madsen JR. The pulsating brain: A review of experimental and clinical studies of intracranial pulsatility. Fluids and barriers of the CNS 2011;8(1):5.

2. Heiss JD, Suffredini G, Smith R, et al. Pathophysiology of persistent syringomyelia after decompressive craniocervical surgery. Clinical article. Journal of neurosurgery Spine 2010;13(6):729-742.

3. Meadows J, Kraut M, Guarnieri M, Haroun RI, Carson BS. Asymptomatic Chiari Type I malformations identified on magnetic resonance imaging. Journal of neurosurgery 2000;92(6):920-926.

TABLES

Table 1: Average CSF APV and AMV (cm/sec± s.d.)

Measurement	Control (n=10)	Pre-surgery (n=10)	Post-surgery (n=10)
Aqueduct APV	6.6 ± 2.3	8.8 ± 3.4	6.4 ± 2.5
Aqueduct AMV	2.6 ± 0.9	3.8 ± 1.4	1.7 ± 2.4
CVJ (Anterior) APV	10.7 ± 2.0	11.1 ± 8.0	8.5 ± 4.2
CVJ (Anterior) AMV	6.1 ± 1.2	4.3 ± 1.6	1.2 ± 5.7
CVJ (Posterior) APV	6.3 ± 2.0	7.3 ± 3.6	8.1 ± 1.7
CVJ (Posterior) AMV	3.5 ± 1.3	2.3 ± 1.1	1.0 ± 4.7

CSF = cerebrospinal fluid; CVJ = craniovertebral junction

Table 2: Significance tables (p-values) for flow parameters versus group (Student *t*-test).

Measurement	Control vs. Pre-surgery	Control vs. post-surgery	Pre- vs. post-surgery
Aqueduct APV	0.11	0.85	0.09
Aqueduct AMV	**0.03**^{S}	0.63	**0.02**^{S}
CVJ (Anterior) APV	0.88	0.17	0.20
CVJ (Anterior) AMV	**0.01**^{S}	**0.02**^{S}	0.18
CVJ (Posterior) APV	0.49	0.06	0.95
CVJ (Posterior) AMV	0.09	0.17	0.35

CVJ = craniovertebral junction; ^{S} = significant

Table 3: Age of volunteers and patients included in the study

	Volunteers	Pre-Operative	Post-Operative
All	11.4	12.9	14.3
Males	11.7	11.5	13.0
Females	11.0	14.6	15.8

Table 4: Basic patients' demographics and procedures

Sl. No	Age/Sex At time of surgery	Chief complaint	Syrinx	Procedure	Outcome on follow-up study
1	17M	Headaches, snoring, difficulty in swallowing	Cervico-thoracic	Duraplasty	Syrinx Resolved. All symptoms resolved
2	19M	Headache/ Vertigo	Absent	Duraplasty	Complete resolution
3	13F	Headache, Rt facial weakness	Absent	Duraplasty	Symptoms resolved/
4	8F	Headache, ataxia	Cervico-thoracic/	Duraplasty	Syrinx improved
5	13F	Headache Sleep Apnea	Cervical	Duraplasty	Headache resolved/syrinx improved/apnea controlled
6	7M	Headaches	absent	Duraplasty	Headache resolved
7	12F	Headaches	absent	No Duraplasty	Headache resolved
8	16M	Headache and vomiting	absent	No Duraplasty	Headache significantly improved
9	10M	Asymmetric arm pain	Cervical		Arm pain resolved/syrinx resolved
10	20F	Headache	absent	Duraplasty	Headaches substantially improved

Figure Legends

Figure 1. Sagittal T1-weighted MRI of the head and cervical spine, with the neck in the neutral position. Annotations represent the axial plane of phase-contrast CSF flow measurements at the aqueduct and craniovertebral junction in a patient with CMI.

Figure 2 a, b, c Graphical representation of a Q flow output showing amplitude(a), ROI placed over the aqueduct (b) and the anterior/posterior compartments of the CVJ (c).

Figure 3 a and b. Line graphs depicting the average amplitude of peak flow (3a) and amplitude of mean flow (3b) within the cerebral aqueduct, in normal controls and patients before and after decompression CVJ surgery. Note that flow normalizes following surgery.

Figure 1. Sagittal T1-weighted MRI of the head and cervical spine, with the neck in the neutral position. Annotations represent the axial plane of phase-contrast CSF flow measurements at the aqueduct and craniovertebral junction in a patient with CMI..
152x169mm (300 x 300 DPI)

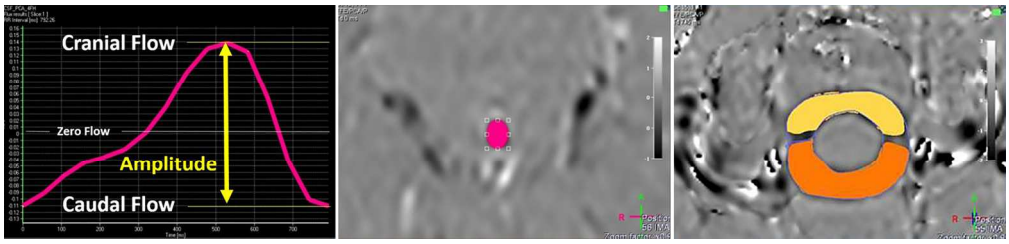

Figure 2 a, b, c Graphical representation of a Q flow output showing amplitude(a), ROI placed over the aqueduct (b) and the anterior/posterior compartments of the CVJ (c).
152x35mm (300 x 300 DPI)